UC Santa Cruz
UC Santa Cruz Previously Published Works

Title

Anticipating fluctuations of bigeye tuna in the Pacific Ocean from three-dimensional ocean biogeochemistry

Permalink

Journal

ISSN

Authors

Taboada, Fernando G
Park, Jong-Yeon
Muhling, Barbara A
et al.

Publication Date

DOI

Copyright Information

Peer reviewed

RESEARCH ARTICLE

Journal of Applied Ecology BRITISH ECOLOGICAL SOCIETY

Anticipating fluctuations of bigeye tuna in the Pacific Ocean from three-dimensional ocean biogeochemistry

Fernando G. Taboada[1,2] | Jong-Yeon Park[3] | Barbara A. Muhling[4,5] |
Desiree Tommasi[4,5] | Kisei R. Tanaka[1,6] | Ryan R. Rykaczewski[6] |
Charles A. Stock[2] | Jorge L. Sarmiento[1]

[1]Atmospheric & Oceanic Sciences Program, Princeton University, Princeton, New Jersey, USA; [2]Geophysical Fluid Dynamics Laboratory, National Oceanic and Atmospheric Administration, Princeton, New Jersey, USA; [3]Department of Earth and Environmental Sciences, Jeonbuk National University, Jeollabuk-do, Republic of Korea; [4]Institute of Marine Sciences, University of California, Santa Cruz, Santa Cruz, California, USA; [5]National Oceanic and Atmospheric Administration (NOAA), Southwest Fisheries Science Center (SWFSC), San Diego, California, USA; [6]National Oceanic and Atmospheric Administration (NOAA), Pacifc Islands Fisheries Science Center (PIFSC), Honolulu, Hawaii, USA

Correspondence
Fernando G. Taboada
Email: fgtaboada@gmail.com

Present address
Fernando G. Taboada, AZTI Marine Research, Basque Research and Technology Alliance (BRTA), Txatxarramendi Ugartea z/g, 48395, Sukarrieta, Spain

Handling Editor: Verena Trenkel

Abstract

1. Subseasonal to decadal ocean forecasting can make significant contributions to achieving effective management of living marine resources in a changing ocean. Most applications rely on indirect proxies, however, often measured at the ocean surface and lacking a direct mechanistic link to the dynamics of marine populations.

2. Here, we take advantage of three-dimensional, dynamical reconstructions and forecasts of ocean biogeochemistry based on a global Earth system model to hindcast and assess the capacity to anticipate fluctuations in the dynamics of bigeye tuna (*Thunnus obesus* Lowe) in the Pacific Ocean during the last six decades. We reconstructed spatial patterns in catch per unit effort (CPUE) through the combination of physiological indices capturing both habitat preferences and physiological tolerance limits in bigeye tuna.

3. Our analyses revealed a sequence of four distinct regimes characterized by changes in the zonal distribution and average CPUE of bigeye tuna in the Pacific Ocean. Habitat models accounting for basin-wide fluctuations in the thermal structure and oxygen concentration throughout the water column captured interannual fluctuations in CPUE and regime switches that models based solely on surface information were unable to reproduce. Decade-long forecast experiments further suggested that forecasts of three-dimensional biogeochemical information might enable anticipation of fluctuations in bigeye tuna several years ahead.

4. *Synthesis and applications*. Together, our results reveal the impact of variability of biogeochemical conditions in the ocean interior on the dynamics of bigeye tuna on the Pacific Ocean, raising concerns about the future impact of ocean warming and deoxygenation. The results also lend support to incorporating subsurface

biogeochemical information into ecological forecasts to implement efficient dynamic management strategies and promote the sustainable use of marine living resources.

1 | INTRODUCTION

Exploited marine fish stocks are experiencing unprecedented changes in environmental conditions as the oceans warm, become more acidic and hypoxic (Barange et al., 2018; Weatherton et al., 2016). These issues raise concerns about the sustainability of marine fisheries, the recovery of over-fished stocks (Costello et al., 2016; Duarte et al., 2020), and pose a challenge to current management practices (Cheung et al., 2009). A decrease in landings is an unlikely but undesired scenario (Costello et al., 2020), motivating development of dynamic management strategies that are able to cope with uncertainties arising from the combined impacts of environmental stressors and human exploitation (Maxwell et al., 2015).

Advanced observing and modelling systems can improve fisheries management through the incorporation of information about the impact of environmental variation on living marine resources (Cheung et al., 2016; Skern-Mauritzen et al., 2016; Schmidt et al., 2019). These systems increasingly provide reliable estimates of conditions in the ocean interior, extending the traditional focus on surface physics to more ecologically meaningful, biogeochemical variables like oxygen concentration, pH, primary productivity and export, or trophic dynamics (Schmidt et al., 2019; Stock et al., 2017). In particular, ocean biogeochemical models are increasingly used not only to reconstruct variation of past ocean conditions or to project long-term climate change and their impact on fisheries (Cheung et al., 2016; Stock et al., 2011), but to develop high quality forecast products at a range of scales, from a few months up to several years in advance (Meehl et al., 2021). These subseasonal to decadal forecasts provide information of high relevance to anticipate fisheries dynamics and to inform decisions in marine resource management (Hobday et al., 2016; Tommasi, Stock, Hobday, et al., 2017). Together, these advances offer the opportunity to incorporate realistic constraints on the distribution and performance of fisheries species into dynamic management systems.

Available studies have developed skillful forecasts of changes in the distribution of marine species from a few hours to a few months in advance (reviewed by Payne et al., 2017). These approaches often rely on training species distribution models to project species occupancy based on lagged relationships with past observations or on dynamical forecasts of surface physical conditions (Hobday et al., 2011; Kaplan et al., 2015). Some of these forecast systems have evolved to operational status with proven value to optimize fisheries profits and reduce negative impacts (Eveson et al., 2015). Forecasts of fish numbers or biomass (Tommasi, Stock, Pegion, et al., 2017; Woodworth-Jefcoats & Wren, 2020), as well as longer lead forecasts incorporating variables other than temperature, are

less common (but see Brodie et al., 2021; Park et al., 2019). There is thus limited understanding of the capacity of biogeochemical information to improve forecasts of living marine resources through the provision of a more direct link to environmental drivers like changes in productivity (Chavez et al., 2003) or oxygen concentration (Stramma et al., 2011).

Here, we develop and assess a forecasting system that takes full advantage of three-dimensional, dynamical reconstructions and predictions of ocean biogeochemistry based on a state of the art Earth system model assimilation and simulation system (Park et al., 2018, 2019). Our analyses targeted large-scale, seasonal to multiannual fluctuations in the abundance and spatial distribution of bigeye tuna, *Thunnus obesus* Lowe, in the Pacific Ocean, where this highly migratory species supports profitable fisheries that have kept detailed, spatial records of catch and effort since 1955. This widely distributed species is sensitive to changes in environmental conditions in the ocean interior, making it a suitable candidate to assess the added value of three-dimensional biogeochemical information. In a first step, we resolve the alternation of consecutive 15- to 20-year-long periods characterized by high or low catch per unit effort (CPUE) of bigeye tuna in the eastern Pacific. We then developed a series of SDMs to assess the utility of biogeochemical data to improve estimates of bigeye tuna catch per unit effort. Our approach relied on the estimation of a series of environmental indices capturing physiological constraints on the distribution and performance of bigeye tuna. We considered environmental indices based either on surface or vertically resolved information, and on variables determined mainly by physical or by biogeochemical processes (e.g. temperature vs. productivity and oxygen). Strikingly, SDMs featuring biogeochemical variables better captured multiannual fluctuations in bigeye tuna and were able to reconstruct regime switches in catch per unit effort. Finally, we combined the resulting SDMs with decade long projections of ocean conditions based on forecast experiments to assess the predictability of fluctuations in bigeye tuna abundance and distribution. The results confirmed the potential added value of incorporating biogeochemical information to improve forecast skill of fisheries models.

2 | MATERIALS AND METHODS

2.1 | *Thunnus obesus* in the Pacific Ocean

Bigeye tuna is a large pelagic schooling fish with a circumglobal distribution that aligns with temperatures of the ocean surface in the 17.0–22.0°C range (Bernal et al., 2017; Block & Stevens, 2001; Brill

et al., 2005; Calkins, 1980; ICCAT, 2006–2016). It is a long-lived, but fast-growing species, with an early maturity (>2 years of age), a mean lifespan of 7–8 years and an adult weight of up to 210 kg. In the Pacific Ocean, two distinct stocks have been defined for the operational management of bigeye tuna fisheries by two separate Regional Fisheries Management Organizations (see inset map in Figure 1). The Inter-American Tropical Tuna Commission (IATTC) manages the eastern stock, and the Western and Central Pacific Fisheries Commission (WCPFC) manages the western stock. Despite the abundance of the population steadily declining since 1950, neither of the two Pacific stocks is considered to be overfished and bigeye tuna supports one of the most profitable fisheries in the Pacific (McCluney et al., 2019; Post & Squires, 2020, but see Xu et al. (2020) for a more concerning reappraisal in the eastern Pacific). The age composition and average size of captures shifted towards young, smaller individuals in the mid 1990s due to the increased use of fish aggregating devices in the purse seine fishery. Total catch remains constant due to the precocious, fast growth and early recruitment of juveniles into the fishery (with recruitment occurring at ages 1 and 0 in the western and eastern Pacific, ICCAT, 2006–2016).

As with most pelagic fishes, bigeye tuna presents a complex life cycle featuring an initial period of high mortality when tiny planktonic eggs and larvae passively disperse in the epipelagic zone. Spawning occurs during the entire year mainly along the equator (Reglero et al., 2014), at temperatures above 24°C (e.g. Schaefer, 2010). Equatorial upwelling fuels enhanced production with respect to subtropical waters, and fosters rapid growth and decreased natural mortality (Lehodey et al., 2008). As a consequence, fish numbers and fisheries catches are higher around the equator. There is also a marked zonal gradient in abundance featuring a one order of magnitude increase in longline CPUE towards the eastern Pacific (Bigelow et al., 2002). These differences in abundance align with an increasing west-to-east gradient in primary productivity and the compression in the vertical habitat of the species and their prey due to the shallower oxygen minimum zone in the eastern Pacific.

As bigeye tuna grow, they develop a characteristic diel vertical migration pattern in open waters away from the coast or seamounts, and when they are not associated to floating objects like fish aggregating devices (Holland et al., 1992). Their diel migration follows, to a large extent, the movement of preferred food resources (i.e. squid and small fishes; Olson et al., 2016), which lead them to dive to depths from 300 to 600 m during daytime in the eastern and western Pacific, respectively, and to feed close to the surface at night (depths about 50 m; Brill et al., 2005). Diel migration is thus closely tied to the position of the deep scattering layer (Dagorn et al., 2000; Schaefer & Fuller, 2010), although daytime excursions also show a characteristic 'u-shaped' pattern that emerges from the alternation of long spans at depth with rapid excursions towards shallow waters to warm-up and recover from the exposure to low oxygen conditions (Holland et al., 1992; Musyl et al., 2003; Thygesen et al., 2016).

Bigeye tuna has the largest tolerance to hypoxia among tunas (Lowe et al., 2000), but oxygen availability still constrains feeding and thermoregulation (Brill et al., 2005). There are occasional recordings of adult bigeye tuna diving to depths below 1000 m in hypoxic waters with $1.0\,\mathrm{mL_{O_2}\,L^{-1}}$ (Schaefer et al., 2009), but feeding excursions rarely extend to waters with oxygen levels below $2.0\,\mathrm{mL_{O_2}\,L^{-1}}$ (Brill et al., 2005). Tolerance to low oxygen concentration rests on the high oxygen-binding affinity of the blood of bigeye tuna during ventilation through the gills, but also on its unique ability to release oxygen at active tissues adapted to sustain high metabolic rates at temperatures above those of deep seawater (Bernal et al., 2017). Such adaptation constrains bigeye tuna to maintain deep body temperatures above 17–18°C for proper tissue oxygenation, temperatures that bigeye tuna keep through active behavioural thermoregulation with short warm up excursions to shallow waters during its vertical migration (Bernal et al., 2017; Musyl et al., 2003). As a consequence, vertical habitat extent often maps closely to the depth of the 10°C isotherm, which provides a lower threshold temperature for bigeye tuna distribution (Brill et al., 2005; Holland et al., 1992).

Migratory behaviour is not restricted to the vertical. Although bigeye tuna tends to remain close to their natal territory, multiple observations support the active movement of individuals across the Pacific at seasonal to annual scales (Rooker et al., 2016). Such observations suggest the existence of several interconnected subpopulations (Schaefer et al., 2015). Evidence for the active connectivity among the western and eastern Pacific fuels discussion about the spatial structuring of the population and about the appropriateness of subdividing it for management purposes (Ducharme-Barth et al., 2020). Here, we separately replicated all analyses for the eastern and western stocks (corresponding to IATTC and WCPFC commissions) to assess whether there are differences in their temporal dynamics. We also test our results under the current management scheme and also considered a single population combining data from both stocks.

2.2 | Analysis of trends and identification of distinct regimes

We focused our analysis on publicly available IATTC and WCPFC databases of tunas and billfishes. These provide monthly longline catch records aggregated over a $5°\times5°$ grid that enabled us to define a nominal annual CPUE index based on the total number of captures divided by the total number of longline hooks set. Longline data are one of the main inputs to stock assessments of large pelagic species and provide information about changes in the overall abundance and spatial distribution of bigeye tuna. The nominal CPUE gives a simple index of relative abundance but it is important to stress its limitations, which mainly arise from the difficulty of characterizing changes in catchability (see e.g. Maunder et al., 2006). For example, a simple effort metric like the number of hooks is affected by variability in catchability under different environmental conditions (e.g. Bigelow et al., 2002; Sharp, 1978), and changes in the number of hooks allowed between floats and other fisheries regulations (e.g. Xu et al., 2020). Assumptions about changes in catchability can even lead to contrasting inferences about trends in population abundance (e.g. compare Myers & Worm, 2003 and Sibert et al., 2006).
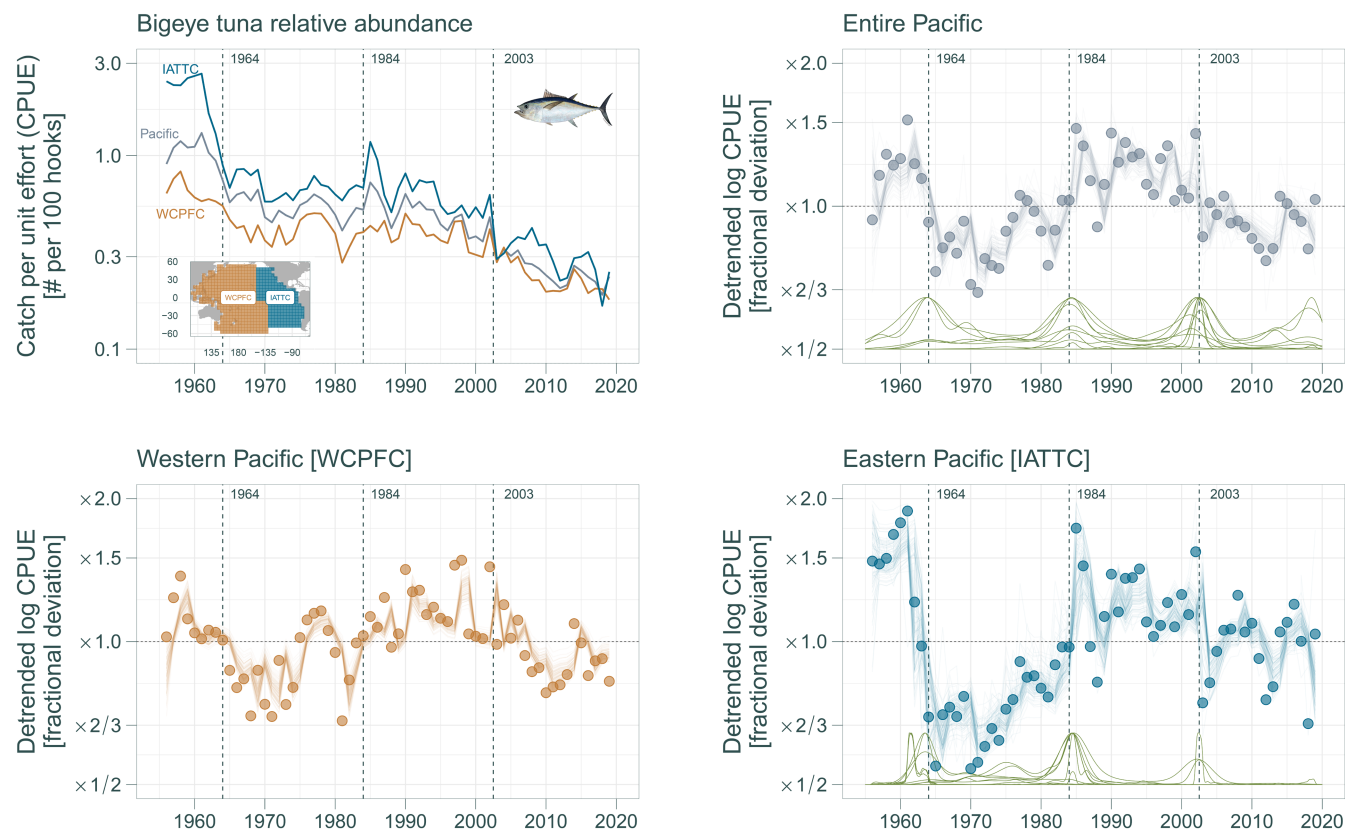
FIGURE 1 Analyses of regime switching behaviour in time series of bigeye tuna CPUE in the Pacific Ocean based on a changepoint model. The analysis delimited four distinct periods and suggests the presence of a multi-annual to decadal signal in the CPUE of bigeye tuna in the Pacific Ocean that may be predictable. The upper left panel shows the natural logarithm of the area-weighted average of CPUE for the entire basin, and for the western and eastern Pacific stocks (the inset map depicts the areas used for aggregation: WCPFC stands for Western and Central Pacific fisheries commission and IATTC is the inter-American tropical tuna commission). The other plots present the predictions of the best regime switching models (see Table 1), which were fitted to the CPUE time series after removing its linear trend (i.e. a constant rate decay process of $\sim 2\%\,\text{year}^{-1}$ that we assumed was due to fishing). The dots correspond to observations and the lines show posterior model fits; the green lines in the bottom axis reflect uncertainty about the location changepoints. Note that model selection favoured no regime switchs in the WCPFC area.

It is also important to note that the longline fisheries capture mainly adults (≥2 years in age and 80–180 cm in size), whereas juveniles are captured by purse seiners. The latter now account for up to two thirds of the catch during the last two decades, an increase that contributes to total catch being stable at 260×10^3 metric tonnes per year in the Pacific since the late 1990s. Despite changes in regulations and gear configuration through the years, the longliner data set provides an almost homogeneous coverage for the entire basin since the early 60s that enabled our analyses herein.

Time series of area-weighted average show a sustained decline in the CPUE of bigeye tuna between 1950 and 2017 in the Pacific (Figure 1). Such decline, which we assumed to be primarily a consequence of overexploitation (e.g. Juan-Jorda et al., 2011), is the most prominent feature of the series and accounts for $\sim 80\%$ of the variability of bigeye tuna CPUE (there is a similar, parallel trend in the biomass caught per unit effort by the longline fisheries). Detrended time series suggest the presence of well-defined modes in the residuals due to prolonged fluctuations above and below the mean state dictated by the overall trend (Figure 1). Such patterns are consistent with the alternation of distinct regimes in the CPUE of bigeye

tuna in the Pacific separated by abrupt transitions. The aim of our historical reconstructions and forecast experiments was to identify the environmental drivers behind such fluctuations and assess their potential predictability.

We examined the presence of alternative regimes through change point analysis (Lindeløv, 2020) of CPUE time series, starting with a null model assuming just first-order autoregressive dynamics and progressively testing models considering up to six regime switches in the overall mean (Table 1). Alternative models were fitted using Markov chain Monte Carlo methods (e.g. Gelman et al., 2014) in *R* (v. 4.0.5) using the package MCP (Lindeløv, 2020), which implements regression based multiple change point models through the software JAGS (Plummer, 2003). We kept the default uninformative priors for model coefficients and change points (Lindeløv, 2020).

Inference was based on 5000 posterior samples following 10,000 iterations for adaptation to ensure convergence, which we further assessed through visual inspection of trace plots and checking that Gelman and Rubin's (1992) diagnostic resulted in values close to unity. Then we calculated Watanabe's information criterion (Watanabe, 2013) to rank alternative models based on their ability

TABLE 1 Model selection table for the changepoint analysis. Each model features first-order, autoregressive errors and allows for changes in the mean and in the correlation structure of the series (Lindeløv, 2020). We took the natural logarithm of the area-weighted average of catch per unit effort in the entire basin prior to the analyses and removed a linear trend from the resulting time series (i.e. a constant rate decay process we assumed it is due to fishing). The first column gives the number of changepoints considered by each model (n_{cp}). The rest of the columns provide separately for each region the metrics involved in model selection: ELP is the expectation of the logarithm of pointwise predictive density and provides a measure of model skill analogous to the log likelihood (ELP) and complexity ($p_{W_{AIC}}$) to guide model selection; ΔW_{AIC} is the deviation of W_{AIC} with respect to the value for the best model; and w_i is a relative weight reflecting the support received by each model based on W_{AIC} values. See Section 2.2 for further details

n_{cp}	Pacific Ocean					Western Pacific (WCPFC)					Eastern Pacific (IATTC)				
	ELP	$p_{W_{AIC}}$	W_{AIC}	ΔW_{AIC}	w_i	ELP	$p_{W_{AIC}}$	W_{AIC}	ΔW_{AIC}	w_i	ELP	$p_{W_{AIC}}$	W_{AIC}	ΔW_{AIC}	w_i
Null	29.5	2.9	−58.96	4.40	0.05	30.9	2.8	−61.87	0.00	0.22	7.2	4.0	−14.47	9.61	0.00
1	28.6	6.3	−57.13	6.23	0.02	30.4	4.5	−60.86	1.01	0.13	6.3	10.3	−12.65	11.44	0.00
2	28.3	10.4	−56.59	6.77	0.01	30.6	7.2	−61.16	0.71	0.16	6.5	15.0	−13.00	11.08	0.00
3	29.8	11.8	−59.67	3.69	0.06	30.7	8.6	−61.45	0.42	0.18	8.5	17.6	−17.06	7.03	0.01
4	31.7	11.4	−63.36	0.00	0.41	30.3	10.1	−60.52	1.35	0.11	12.0	16.2	−24.08	0.00	0.37
5	31.3	13.9	−62.65	0.71	0.29	30.2	11.6	−60.40	1.46	0.11	11.7	18.1	−23.44	0.64	0.27
6	30.8	14.4	−61.51	1.85	0.16	30.0	12.9	−60.03	1.84	0.09	11.9	18.8	−23.89	0.19	0.34

to predict observations at the lowest model complexity (Hooten & Hobbs, 2015). The model with the lowest Watanabe's information criterion provided a sequence of turning points defining alternative regimes that were used to group the data and assess the ability of SDMs to reproduce fluctuations in the dynamics of bigeye tuna.

2.3 | Biogeochemical data

To analyse the impact of environmental variability on bigeye tuna CPUE in the Pacific Ocean, we took advantage of the 1960–2017 ocean reanalysis and decade-long forecast experiments provided by the Ensemble Coupled Data Assimilation system integrating the Carbon, Ocean Biogeochemistry and Lower Trophics biogeochemical model (ECDA-COBALT; Park et al., 2018, 2019). The system combines a global coupled climate model with an ensemble Kalman filter to assimilate physical observations (both atmospheric temperature and wind, and the temperature and salinity of the ocean surface and its interior; see Zhang et al., 2007). The system also includes the biogeochemical model COBALT to resolve pelagic nutrient cycles and carbon and energy fluxes through the planktonic food web (Stock et al., 2014). Integration of COBALT with the data-assimilative physical fields yielded improved representations of simulated temperature, oxygen, nutrient and chlorophyll fields critical to bigeye tuna habitat (Park et al., 2018).

Simulated, three-dimensional fields were retrieved for both physical (temperature and salinity) and biogeochemical variables (oxygen concentration and primary production). ECDA-COBALT simulated the dynamics of ocean fields over a grid with a horizontal resolution of 1° telescoping to 1/3° meridional extent towards the equator, and 50 vertical levels of varying thickness (i.e. from 10 m near the surface to 400m in the abyssal zone). We used first order conservative interpolation to align the original data with the coarser 5°×5° grid adopted by IATTC and WCPFC to aggregate bigeye tuna data. As described below, it was necessary to apply customary adjustments to correct model drift in the case of decade long forecasts experiments (see below; no adjustments were applied to the reanalysis fields). In both cases, we calculated the average of 12 ECDA-COBALT ensemble members.

2.4 | Reconstructing and forecasting bigeye tuna CPUE

2.4.1 | Environmental covariates and habitat quality indices

We calculated five complementary indices to capture environmental constraints on the distribution of bigeye tuna. We considered first the two ocean physical conditions most often cited to describe the horizontal distribution of bigeye tuna (Section 2.1); (i) the temperature of the ocean surface (tos[°C]), and (ii) the depths of the 10°C isotherm ($z_{10°C}$[m]), which often align with bigeye tuna daytime feeding

depths (e.g. Brill et al., 2005). We expect both to show a unimodal relationship with bigeye tuna abundance anomalies throughout the Pacific Ocean during the study period. For *tos*, we expect the correlation among surface temperatures and the extent of bigeye tuna distributional range to set an intermediate optimum. In the case of $z_{10°C}$, we expect a decline in CPUE both for too shallow and too deep vertical habitat extents, which are indicative of either unfavourable temperate conditions, or strongly stratified, oligotrophic waters requiring long, low reward deeper feeding excursions, respectively.

Next we considered three additional indices based on compound biogeochemical variables emerging from the interaction of ecosystem dynamics with physical and chemical forcing: (iii) net primary production (NPP [$mg\,cm^{-2}\,day^{-1}$]); (iv) average partial pressure of oxygen in the mesopelagic zone (pO_2^{meso} [kPa]), defined between 300m and 600m to approximately match the vertical range of bigeye tuna diel migrations; and (v) the depth of the ambient oxygen partial pressure resulting in a 50% saturation of bigeye tuna whole blood ($z_{p_{50}}$ [m]).

To first order, we expect a positive, possibly saturating effect of higher net primary production on bigeye tuna abundance through direct trophic transfer. The two oxygen indices attempt to capture three-dimensional habitat suitability constraints, and their calculation was based on oxygen partial pressures, accounting for the effect of temperature, salinity and hydrostatic pressure on oxygen solubility (Enns et al., 1965; García & Gordon, 1992). The second oxygen index considered, $z_{p_{50}}$, is based on the tolerance of bigeye tuna to low oxygen concentration (see Section S1 in the Supplement for full details about its calculation). It has been proposed as an index to characterize vertical habitat extent for mesopelagic species and has been used it to project potential changes in the habitat of commercially exploited tuna species due to climate change (Mislan et al., 2017). We expect higher pO_2^{meso} concentrations and deeper $z_{p_{50}}$ to correspond to an extended vertical foraging habitat for bigeye tuna, and thus to be positively correlated with CPUE.

The two oxygen indices provide complementary information about changes in habitat suitability for bigeye tuna; mesopelagic oxygen concentration targets smooth changes in vertical distribution and performance, while the isopleth of whole blood half-saturation targets physiological threshold responses that may lead to sharp distributional shifts. The indices are further correlated with the position of the deep scattering layer (e.g. Aksnes et al., 2017) during daytime and thus with the approximate extent of bigeye tuna vertical migrations. These two indices provide information about habitat extent and quality, including the vertical compression expected as a consequence of climate change (Stramma et al., 2011), which is especially apparent in the eastern Pacific Ocean (Breitburg et al., 2018; Deutsch et al., 2014).

2.4.2 | Habitat reconstructions based on Earth system model hindcast experiments

We developed a set of semi-mechanistic SDMs to reconstruct the spatiotemporal dynamics of bigeye tuna in the Pacific Ocean between 1960 and 2017 based on the habitat quality indices derived from

reconstructed biogeochemical fields estimated by ECDA-COBALT (see Sections 2.3 and 2.4.1 above). We conducted our analyses using generalized additive models (GAMs; Hastie & Tibshirani, 1986; Wood, 2017) with varying combinations of the environmental indices outlined above. These same models were later used to forecast bigeye tuna CPUE up to 10 years in advance (see below). The defining feature of GAMs is that they enable the characterization of the relationship among response and predictor variables through a set of unspecified smooth functions (i.e. here, thin plate regression splines with a degree of smoothness determined by a quadratic penalty (Wood, 2016, 2017)). This approach enabled our models to capture nonlinear effects and threshold responses to environmental drivers.

We trained models considering different subsets of habitat quality indices that align through two axes: indices representing conditions close to the surface versus vertically resolved information (depth of selected isopleths or properties averaged throughout the water column), and indices based on physical variables (i.e. temperature) versus indices incorporating biogeochemical information (i.e. primary production and oxygen; see Section 2.4.1 above and Table 2). We assessed model predictions against observations of bigeye tuna CPUE, focusing on the ability of alternative models to reproduce changes in spatial distribution and fluctuations in average CPUE. In this way, we progressively assessed the value of depth-resolved and biogeochemical information relative to the surface values often relied upon for SDM applications (e.g. Pickens et al., 2021).

The set of candidate models were used to explain spatial and temporal variability observed in the time series of the natural logarithm of longline catch per unit effort, $x_{t,s} = logCPUE_{t,s}$ [count + 1 per 10^4 hooks], averaged for each year t and for each $5° \times 5°$ cell location s. The natural logarithm transformation approximated residuals to be independent and identically distributed normal errors. We added the minimum observed abundance (i.e. one individual caught) to each CPUE observation to avoid undefined logarithms, following advice in Turchin (2003). All the SDMs shared a common frame featuring a null model with a linear trend and a lagged density dependent effect;

$$x_{t,s} = \alpha + \beta \times t + \gamma \times \overline{x_{t-1,\bullet}}, \tag{1}$$

where α, β, and γ are constant parameters and $x_{t-1,\bullet}$ is the average CPUE anomaly in the previous year, calculated as the logarithmic deviation from the decaying trend due to fishing.

The null model represents the null hypothesis of no environmental effects on observed fluctuations in bigeye tuna CPUE. It accounts however for the overall decline in relative abundance due to fishing, which we introduced through a constant rate geometric decay process ($\beta \times t$, where t is time in years). It also allows for short range population fluctuations through a delayed density dependent effect on the average abundance anomaly over the species range during the previous year ($\overline{x_{t-1,\bullet}}$). Defining α as the intrinsic growth rate (year^{-1}) and γ [−] as a parameter measuring the strength of density dependence, these terms correspond to a linearized, discrete time Gompertz model for a closed population where the equilibrium

TABLE 2　Model selection table for the analysis of changes in bigeye tuna CPUE in the Pacific Ocean using species distribution models (SDMs). The table presents the hypothesis underlying each SDM and the corresponding covariates included on each generalized additive model (GAM), where the terms $f(\bullet)$ correspond to unspecified smooth functions of the predictor variables. The SDMs target the natural logarithm of bigeye tuna abundance, $x_{t,s} = \log\mathrm{CPUE}_{t,s}$, averaged during year t for each $5° \times 5°$ grid cell location. We used the capital letter $\mathcal{N}$ to refer to the null component shared by all models. Predictors can be classified either as physical ($\mathcal{P}$) or biogeochemical ($\mathcal{B}$) indices, and as surface ($\mathcal{S}$) or vertically resolved ($\mathcal{V}$) indices. Please note that we omitted the subscripts for the environmental covariates, although they also varied in space and time. The rest of the columns provide the metrics involved in model selection: ELP is the expectation of the logarithm of pointwise predictive density and provides a measure of model skill analogous to the log likelihood function (the higher the better); $p_{W_{\mathrm{AIC}}}$ is the effective number of parameters which gives a proxy model complexity, W_{AIC} is Watanabe's information criterion (Watanabe, 2013), which accounts for model skill (ELP) and complexity ($p_{W_{\mathrm{AIC}}}$) to guide model selection; ΔW_{AIC} is the deviation of W_{AIC} with respect to the value for the best model; w_i is a relative weight reflecting the support received by each model based on W_{AIC} values; and $\left(1 - \frac{D}{D_0}\right)$ is the fraction of deviance explained by each model

Model for $x_{t,s} = \log\mathbf{CPUE}_{t,s}$	ELP	$p_{W_{\mathbf{AIC}}}$	$W_{\mathbf{AIC}}$	$\Delta W_{\mathbf{AIC}}$	w_i	$1 - D / D_0$
Null model						
$\quad x_{t,s} = \alpha + \beta \times t + \gamma \times \overline{x_{t-1,\bullet}} = \mathcal{N}$	−43,159.8	4.8	86,319.63	12,832.30	0.00	0.04
Physical indices						
$\quad x_{t,s} = \mathcal{N} + f(tos)$	−40,806.5	11.0	81,613.05	8125.72	0.00	0.23
$\quad x_{t,s} = \mathcal{N} + f(z_{10°C})$	−40,682.2	10.8	81,364.48	7877.16	0.00	0.24
$\quad x_{t,s} = \mathcal{N} + f(tos) + f(z_{10°C}) = \mathcal{N} + \mathcal{P}$	−39,276.4	18.7	78,552.81	5065.48	0.00	0.34
Biogeochemical indices						
$\quad x_{t,s} = \mathcal{N} + f(NPP)$	−42,559.7	9.6	85,119.47	11,632.14	0.00	0.10
$\quad x_{t,s} = \mathcal{N} + f(z_{p_{50}})$	−42,639.3	14.0	85,278.57	11,791.25	0.00	0.09
$\quad x_{t,s} = \mathcal{N} + f(pO_2^{meso})$	−40,402.1	11.5	80,804.15	7316.82	0.00	0.26
$\quad x_{t,s} = \mathcal{N} + f(z_{p_{50}}) + f(pO_2^{meso})$	−39,954.0	20.8	79,908.06	6420.74	0.00	0.30
$\quad x_{t,s} = \mathcal{N} + f(NPP) + f(z_{p_{50}}) + f(pO_2^{meso}) = \mathcal{N} + \mathcal{B}$	−39,527.5	26.7	79,054.95	5567.62	0.00	0.32
Surface vs. vertically resolved indices						
$\quad x_{t,s} = \mathcal{N} + f(tos) + f(NPP) = \mathcal{N} + \mathcal{S}$	−40,139.6	16.5	80,279.28	6791.95	0.00	0.28
$\quad x_{t,s} = \mathcal{N} + f(z_{10°C}) + f(z_{p_{50}}) + f(pO_2^{meso}) = \mathcal{N} + \mathcal{V}$	−38,158.7	27.7	76,317.32	2829.99	0.00	0.41
All indices						
$\quad x_{t,s} = \mathcal{N} + \mathcal{P} + \mathcal{B} = \mathcal{N} + \mathcal{S} + \mathcal{V}$	−36,743.7	40.8	73,487.32	0.00	1.00	0.48

density decays due to fishing pressure (e.g. Dennis & Taper, 1994). For simplicity, the null model assumes a homogeneous effect of density dependence throughout bigeye tuna range, which ignores the heterogeneous mixing within the population (Schaefer et al., 2015).

The null model provided a simple baseline to test potential improvements in predicting bigeye tuna CPUE through the incorporation of the effect of different sets of environmental drivers. As detailed in Table 2, we extended the null model by considering first a subset of models featuring different combinations of either physical or biogeochemical variables. We then considered two extra models combining information about the state of the surface ocean versus vertically resolved variables, without distinction of their physical or biogeochemical nature. Finally, we added a 'saturated' model featuring all environmental effects. Although not entirely independent, this design enabled us to assess the potential gain in skill with respect to the null model associated with each of the different covariates, and to compare target subsets corresponding to hypotheses about the importance of environmental effects of different nature. We examined model residuals to check model assumptions and to assess the performance of alternative models using the same model selection detailed above (Section 2.2).

All the analyses were performed in R version 4.0.5 (R Core Team, 2021); GAMs were fitted using Bayesian methods with the *jagam* interface to JAGS (Plummer, 2003; Wood, 2016), which is available through the package MGCV (Wood, 2017). This approach enabled us to propagate uncertainty from model parameterization to model assessment and selection. To do that, we took 1000 posterior samples with a thinning interval of 10, following an adaptation plus warmup period of 20,000 iterations. We set weakly informative conjugate priors following Wood (2016) to ensure convergence, which was further assessed through visual inspection of trace plots and checking that estimated of Gelman and Rubin's (1992) diagnostic were close to unity. The algorithm sets standard GAM estimates as starting points for the MCMC procedure, which ensures a rapid convergence. Model selection was conducted using Watanabe's information criterion to rank alternative models.

2.4.3　│　Retrospective forecast experiments

We concluded our analysis by providing an initial assessment of the ability of Earth system model predictions to improve the skill of

forecasts of bigeye tuna CPUE. The design paralleled the approach followed above to assess reconstructions of past variability in bigeye tuna CPUE, but physical-biogeochemical forecasts (Park et al., 2019) replaced the reanalysis during the forecast period. The forecasts start at the beginning of each year between 1960 and 2017 and run free for an entire decade. The SDMs featured the same annual environmental indices to repeat our calculation of the added skill contributed by physical versus biogeochemical information, and by surface versus vertically resolved data for the forecast period. Density dependent effects were dynamically updated based on the previous year forecasts for lead times longer than 1 year, and the geometric decay in abundance was propagated based on the last available estimate.

Deviations from a realistic scenario included the use of SDMs trained with data available during the entire study period instead of conducting an online update mimicking how information became available in the past. This choice reflects constraints imposed by the limited duration of the time series relative to low frequency fluctuations identified in our analyses (Section 3.1) and avoids the computational cost of fitting the comprehensive sequence of GAMs considered herein for a multitude of distinct data combinations. The resulting predictability assessment must be viewed, however, as providing an upper skill bound that may not be reached.

To assess the extra skill gained by each combination of environmental indices, we focused on the ability of alternative models to reconstruct fluctuations in the overall CPUE of bigeye tuna in the Pacific Ocean. We detrended the resulting series and calculated 3 years moving averages to match the triennial scale of stock assessments for the fishery. To avoid spurious effects, we sampled the forecasts at the same locations and times as available CPUE data. Then, we calculated for each SDM in Table 2 and each lead time the anomaly correlation coefficient (ρ), mean absolute deviations, and the mean absolute scaled error (Hyndman & Koehler, 2006) between the observed and forecast 3-year averaged CPUE. Anomaly correlations were estimated using Pearson product moment correlations. Mean absolute deviations complement the assessment by providing the magnitude of average forecast errors. Lastly, mean absolute scaled errors give the average relative error with respect to that resulting from a naïve, random walk forecast (i.e. just using the last available observation to predict the future). Values below unity correspond to forecasts beating the benchmark set by the naïve forecast. We provide full details about the forecast experiments in Section 1.2 in the Supplement.

The study did involve neither the manipulation nor any experiment with animals or humans, and it did not require ethical approval.

3 | RESULTS

3.1 | Decay trend and emergence of regime shifts

Longline CPUE time series showed a sustained decline of $\sim 2\% \, \text{year}^{-1}$ in the abundance of bigeye tuna between 1950 and 2017 presumably due to commercial exploitation (Juan-Jorda et al., 2011; Figure 1).

Log-linear detrending revealed, however, a sequence of prolonged periods spanning up to two decades characterized by sustained fluctuations above and below the prevailing negative trend (Figure 1). Analyses using change point models confirmed the presence of four distinct regimes of bigeye tuna in the Pacific (Table 1 provides relative model weights). High anomalies relative to the prevailing decline were apparent at the start of the series (1958–1964) and between 1984 and 2003, while low anomalies were evident between these two periods and after 2003. The same periods and switching dates (1964, 1984 and 2003) emerged for the eastern Pacific CPUE series, but not for the west, where a null model featuring just red noise cannot be dismissed (see e.g. Rudnick & Davis, 2003), even if the three anomaly time series were highly correlated ($r > 0.8$).

3.2 | Habitat reconstructions

The distinction of four consecutive periods helped us to frame the rest of the analysis. Periods of high versus low bigeye tuna CPUE relative to the long-term decline corresponded to zonal changes in the distribution along the eastern versus western Pacific Ocean (Figure 2). These changes have been previously reported and ascribed to the concentration of the population towards the eastern equatorial Pacific in response to warm surface conditions like those associated with El Niño-Southern Oscillation Modoki (ENSO Modoki) of 1963 (e.g. Kume & Schaefer, 1966). In contrast to canonical El Niño events, ENSO Modoki years are characterized by warm surface conditions in the central Pacific and cool anomalies in the eastern and western Pacific (Capotondi et al., 2020). Habitat reconstructions based on ECDA-COBALT reanalysis suggested instead that changes in bigeye tuna CPUE anomalies rather reflect variability in biogeochemical conditions in the ocean interior (Table 2).

Although model selection favoured the SDM including all habitat quality indices (i.e. the 'saturated' model; see Figure S1 for the estimated partial effects), the skill of habitat reconstructions varied markedly among alternative models (Table 2). These differences can be used to diagnose the contribution of different habitat factors to observed fluctuations around the declining CPUE trend. The saturated, full model captured approximately half of the observed variation. Environmental covariates were behind most model skill, with a negligible contribution from the null model component. Models featuring just physical or biogeochemical habitat quality indices captured only one third of the observed variation (Table 2). The two sets of indices were largely complementary, and the inclusion of biogeochemical indices increased the amount of deviance explained by the saturated model by at least 15% (i.e. one-third of the total fraction of deviance explained). Perhaps most important, only those models incorporating how increases in oxygen concentration at depth favour bigeye tuna were able to reproduce, to some extent, observed zonal changes in CPUE anomalies along the equatorial Pacific, especially the negative anomalies observed in the eastern Pacific during periods below the declining trend (1964–1983 and 2003–2017; Figure 1, and Figures S2–S5).
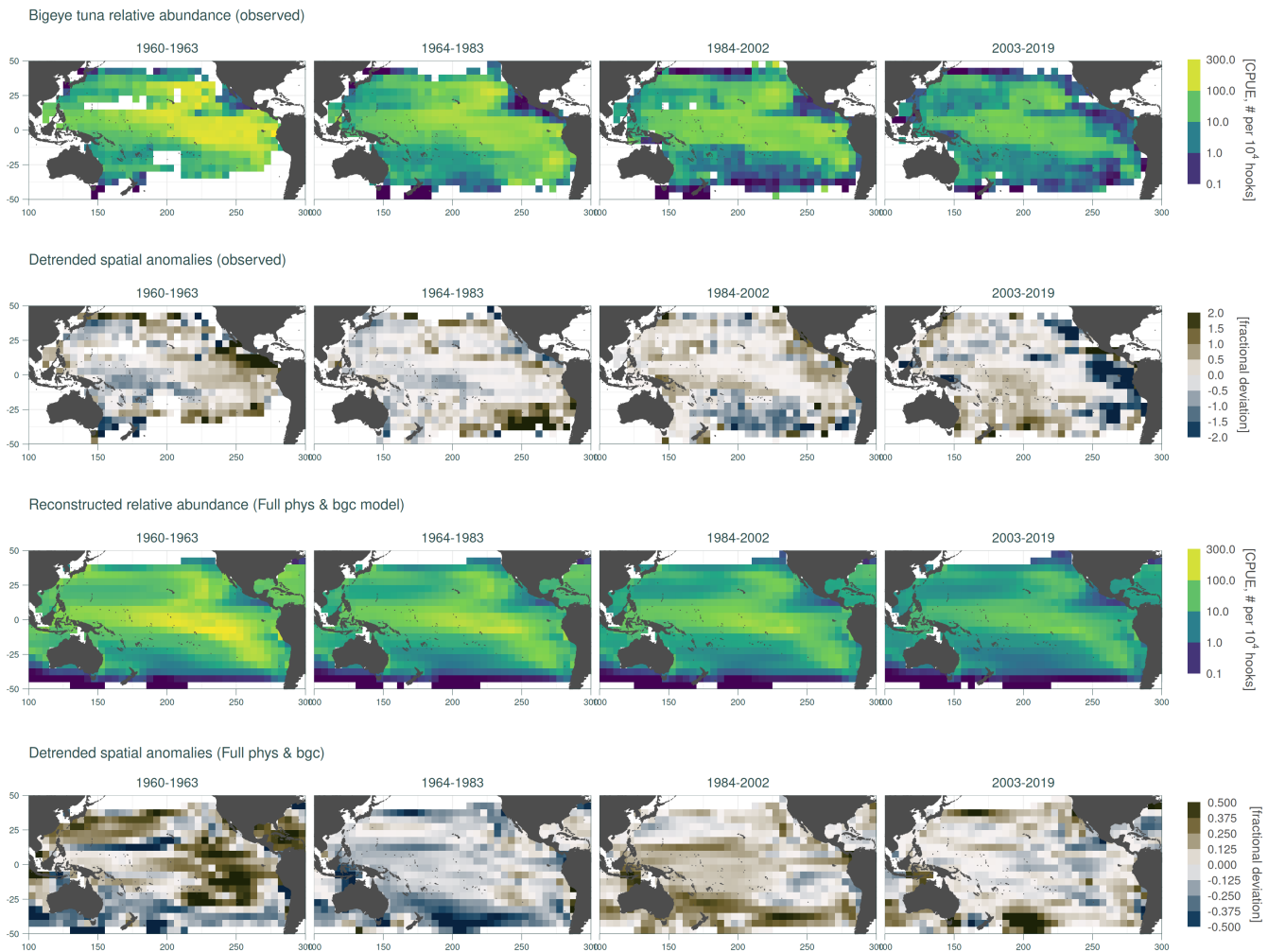
FIGURE 2 Changes in spatial distribution of bigeye tuna in the Pacific Ocean during each of the four periods identified using changepoint analysis Figure 1. Relative abundance was estimated from CPUE ($\times 10^4$ hooks set) based on data retrieved from IATTC and WCPFC databases. Anomaly maps show average deviations during each period from the climatology of linearly detrended deviations of the natural logarithm of CPUE. We present here reconstructed patterns based on the saturated species distribution model (SDM) featuring three-dimensional, biogeochemical variables simulated by GFDL-ECDA-COBALT (Park et al., 2018, 2019); similar plots were prepared for the supplement (i.e. Figures S2–S5). Note the change of scale among the maps featuring spatial anomalies, adjusted to account for the tendency of SDMs to smooth out variability with respect to observations.

Comparison of SDMs featuring habitat indices based on surface versus vertically resolved information further supported the importance of conditions within the ocean interior to reliably predict changes in CPUE anomalies (Table 2). Vertically resolved physical and biogeochemical indices were also complementary and together accounted for up to ~85% of the total variability explained by the saturated full model. These models furthermore reproduced aspects of the zonal changes in bigeye tuna CPUE thanks to the inclusion of oxygen indices (i.e. SDMs only featuring physical indices show either homogeneous (*tos*) or opposite ($z_{10°C}$) zonal patterns to those observed; Figures S3 and S5). Time series based on the SDM habitat reconstructions featuring vertically resolved water column information also provided the best hindcast, even being superior to the saturated SDM model combining all habitat quality indices (Figure S6).

3.3 | Bigeye tuna forecast experiments

Forecast experiments produced in some cases reasonable predictions up to several years in advance that yielded modest but encouraging positive correlations $\rho \approx 0.3 - 0.5$ (Figure 3). As expected, skill varied with lead time and depended on the subset of habitat quality indices included in each SDM (Figure 4; see Figure S8 for complementary skill metrics). The SDMs featuring purely physical habitat quality indices presented the best performance for short term lags up to 3 years. The skill of forecasts based on SDMs featuring only biogeochemical indices increased steadily towards longer lead times. The model featuring only biogeochemical indices was even able to anticipate the transitions among regimes of relative high and low bigeye tuna CPUE, but only a few years in advance. In both cases, forecast skill emerged mainly from the inclusion of vertically resolved

Realized prediction for bigeye tuna in the Pacific Ocean

FIGURE 3 One-to-10 year lead forecasts of bigeye tuna CPUE in the Pacific Ocean. Forecasts are based on species distribution models (SDMs; see Table 2 and Section 2.4.3 for details) forced by environmental fields produced by ECDA-COBALT (see Section 2.3). The SDMs were fitted using all available data during the study period, including both previous year CPUE anomalies and assimilated ECDA-COBALT fields. CPUE was forecast using SDMs forced by ECDA-COBALT forecasts of ocean conditions, and dynamically updated density dependent effects based on the previous year forecasts for lead times above 1 year. The model tends to drift with lead time and to smooth out variabilty in bigeye tuna CPUE, so we subtracted a lead-dependent climatology and centered and rescaled (zero mean, unit standard deviation) the resulting forecasts. The graph shows scaled CPUE data (*blue dots*); the target, 3 year smoothed series (*blue line*); and 10 year lead forecasts initialized each year between 1961 and 2017 (*orange lines*). Similar plots were included in the supplement for the eastern and western Pacific Ocean (Figure S7).

indices and from the ability of the model to capture gear vulnerability in the eastern Pacific Ocean.

The enhanced forecast skill of SDMs featuring biogeochemical versus physical indices at longer lead times is consistent with results suggesting long predictability horizons of biogeochemical variables integrating both surface and subsurface variability (e.g. Park et al., 2019; Seferian et al., 2014); however, the transitions from low skill at short leads to larger correlations at longer leads is counterintuitive. To the best of our understanding, this result reflects both the inability of the model to reproduce short-term variability in CPUE (i.e. SDM based forecasts barely beat the naïve, random walk forecast for lead times up to 3 years), and the longer lasting and predictable evolution of biogeochemical variables at depth versus short term, noisy effects in the surface tightly linked to atmospheric forcing. The ability to forecast surface temperature or NPP was drastically reduced for lead times beyond 1 year in the eastern Pacific Ocean, whereas both oxygen variables and the depth of the 10°C isotherm showed a smooth decay and were more predictable at longer lead times (see Figures S9 and S10 in the Supplement). We caution, however, that even the extremely long catch time series we enlisted offer relatively few independent data points with which to assess predictions. This challenge is shared by multiannual prediction efforts for the physical climate systems (Meehl et al., 2021), and emphasizes the value of sustained observations.

Our results illustrate the potential lack of correspondence between those aspects of the environment that are useful to reconstruct and explain past variation versus those that provide the best forecast skill. In order to be useful for forecast, a variable must be itself predictable and an important driver of variability in the CPUE of the targeted resource. The poor performance of forecasts based on the full saturated model illustrates the need to assess carefully a battery of forecast models, possibly including simpler versions of those providing best reconstructions (e.g. Jacox et al., 2020), to identify combinations of variables that are both predictable and have a significant capacity to anticipate changes in vertical and horizontal distributions.

4 | DISCUSSION

The decline in apparent abundance, indexed by longline CPUE of bigeye tuna in the Pacific Ocean hides the alternation of prolonged periods during which CPUE consistently remained above or below the prevailing negative trend due to fishing. Reconstructions of bigeye tuna CPUE featuring biogeochemical reanalysis data suggest that these fluctuations likely reflect changes in the subsurface ocean, especially of oxygen concentrations determining the vertical extent of bigeye tuna feeding habitat in the central and eastern Pacific Ocean. These same biogeochemical variables seem to have some potential
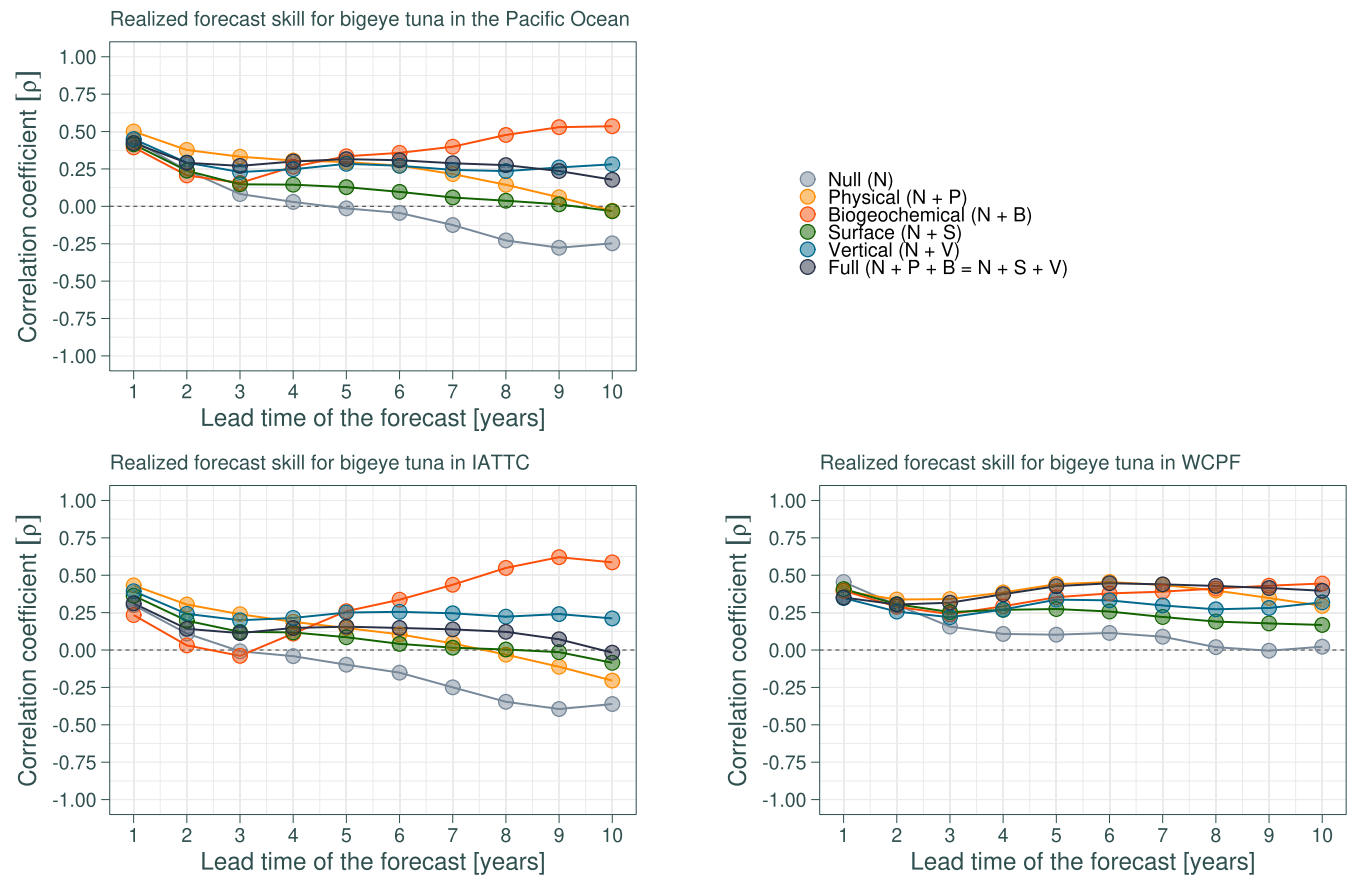
FIGURE 4 Skill of bigeye tuna CPUE forecasts at leads times between 1 and 10 years for the Pacific Ocean and for the subareas corresponding to the eastern (IATTC) and western and central (WCPF) stocks. Forecast skill was assessed using anomaly correlation coefficients; Figure S8 in the supplement presents similar plots featuring complementary skill metrics (mean absolute deviations and mean absolute scaled errors; see Section 2.4.3).

to enable anticipation of long-lasting fluctuations in bigeye tuna CPUE at seasonal to decade-long scales due to their relatively high predictability, at least compared to short-memory surface variables.

The added value contributed by three-dimensional information about the state of the ocean interior to map marine species distributions has been recently highlighted (Bentlage et al., 2013; Duffy & Chown, 2017). Most studies still tend, however, to use primarily surface data and purely physical variables which are more readily available from satellite remote sensing or ocean reanalysis data sets (Pickens et al., 2021). In the case of bigeye tuna and other large pelagics featuring vertical migrations, the importance of three-dimensional information has been long recognized and implemented through ecophysiological constraints on habitat availability and feeding success (e.g. Bernal et al., 2017; Lehodey et al., 2008; Sharp, 1995). Studies incorporating environmental information consistently stress the importance of oxygen concentration and water column thermal structure in determining habitat extent in large pelagics (e.g. Arrizabalaga et al., 2015; Lehodey et al., 2008; Sharp, 1995; Zhang et al., 2021; Zhou et al., 2020). Like in most stock assessments (Skern-Mauritzen et al., 2016), however, management advice mainly relies on the assessment of current status of the stock in relation to reference points, only exploiting short term memory

emerging from changes in size structure at age (e.g. Ducharme-Barth et al., 2020).

Here, a long-term reanalysis of the variability in ocean biogeochemistry during the last six decades enabled us to go a step further and link changes in water column structure to long-lasting fluctuations in bigeye tuna CPUE. Models including metrics related to oxygen concentration at depth and vertical variation in the thermal structure of the water column not only contributed to explain past variability in bigeye tuna, but also resulted in potential predictability over longer time horizons. The identified effects of environmental variables on changes in bigeye tuna CPUE are consistent with known constrains on its physiological performance and behaviour. The saturated model captures the preference for surface waters above 20.0°C and the positive effect of primary productivity and a relatively shallow thermocline depth for prey capture (e.g. Brill et al., 2005; Lehodey et al., 2008). Similarly, the negative effect of low oxygen concentrations is consistent with reported impacts of the vertical compression of habitat and horizontal redistribution of tunas and billfishes (Leung, Mislan, et al., 2019; Stramma et al., 2011).

The enhanced skill of models featuring oxygen metrics and the rapid changes in oxygen variables in the equatorial eastern Pacific about the regime transitions suggest a potential link to patterns

of climate variability associated with ENSO (Leung, Thompson, et al., 2019), augmented by more persistent modes of variability like the Pacific Decadal Oscillation (PDO; Newman et al., 2016). The analyses revealed distinct patterns among the eastern and western stocks. Distinct regimes only emerged in the eastern Pacific Ocean, where biogeochemical indices also contributed to increase forecast skill. Such results probably reflect the greater impact of ENSO on large scale fluctuations in water column biogeochemistry in the eastern Pacific (Capotondi et al., 2020). Warm surface conditions in the eastern Pacific during ENSO events expand favourable habitat for bigeye tuna, promote the formation of high abundance aggregations close to the equator (e.g. Kume & Schaefer, 1966; Lehodey et al., 2008), and promote higher recruitment and increased abundance after a few years (Satoh et al., 2021; Xu et al., 2020).

The regime switches in 1964 and 2003 coincide with the occurrence of central Pacific or «Modoki» ENSO events (Capotondi et al., 2020), which are known to enhance upwelling and anoxia in the eastern Pacific Ocean (Dewitte et al., 2012; Espinoza-Morriberón et al., 2019), and might contribute to explain the onset of low abundance regimes. The switch to high abundances after 1984 follows one of the strongest canonical eastern Pacific ENSO in the record, whose weaker cold phase boosts plankton production and favours bigeye tuna expansion across the equatorial Pacific. Although the regime switches do not match changes in the sign of the PDO in 1977 and 1989 that have been linked to a variety of impacts across the entire Pacific Ocean (Chavez et al., 2003; Hare & Mantua, 2000), the contraction of hypoxic regions and associated expansion of favourable habitat during the positive PDO phase between the late 1970s and early 2000s (Deutsch et al., 2011), and its expansion during the negative cool phase in the 2000s, would help to explain observed fluctuations in the CPUE of bigeye tuna (Figure S10).

The potential link with ENSO events and the PDO also helps to explain the observed increase in prediction skill at longer lead times. Although no forecast system can predict the precise onset of a given ENSO event several years in advance or a phase switch in the PDO (e.g. Meehl et al., 2021), Earth system models have the potential to capture long-lasting effects on water column biogeochemical conditions. For instance, ENSO makes it almost impossible to predict tropical temperature anomalies beyond a year (e.g. Meehl et al., 2021). Variables like primary productivity and subsurface oxygen, on the other hand, often depend on slower ecosystem processes that filter short term variability and result in long-lasting, smooth responses to external perturbations (Park et al., 2019; Seferian et al., 2014; Taboada et al., 2019). Similar smoothing has been observed at higher trophic levels in marine food webs (Barton et al., 2020; Di Lorenzo & Ohman, 2013). Together with longer term trends due to climate change, these smooth responses contribute predictability at longer lead times, while short term scales are dominated by more erratic fluctuations. In the case of bigeye tuna, forecasting changes in vertical habitat extent and primary productivity can impart some predictabilty about bigeye tuna CPUE dynamics 5–10 years in advance. Such information might foster the development of tactical management models to take into account the persistence and alternation of

high and low CPUE regimes. The failure to predict short term fluctuations and the lack of a precise mechanism to explain long-term persistence, however, leaves ample scope to improve our forecasts through a more detailed consideration of inertial effects associated with changes in population age and size structure (Ducharme-Barth et al., 2020), environmental effects on recruitment (Woodworth-Jefcoats & Wren, 2020), and fishing pressure and catchability (Bigelow et al., 2002; Sharp, 1978).

These processes might also be considered additional confounding factors that limit the interpretation of our results. Our semi-mechanistic model features a basic density-dependent term that pools together the impact of changes in abundance and environmental forcing on recruitment, age structure and the productivity of bigeye tuna. There is some evidence of age truncation in bigeye tuna (Ducharme-Barth et al., 2020), which likely reflects the impacts of fishing. It is unlikely, however, that these changes contribute to the observed regime shifts; in the end, bigeye tuna has an early age of maturity (2 years) and preys on short lived species, which together suggests that cohort cycles would rarely exceed a period of 8–10 years (e.g. Murdoch et al., 2002), and fall short to explain observed regime shifts. Trends in the biomass of bigeye tuna are prototypical of large tropical fish species with marked trends associated with the impact of environmental variability and fishing (Taboada, 2019). Age truncation would further promote more erratic, but short-term oscillations in population abundance due to fluctuations in recruitment success (Rouyer et al., 2012). Accounting for these processes, ideally integrated in ecophysiological models informed by dynamic biogeochemical fields (Lehodey et al., 2008; Robinson et al., 2011), may improve knowledge about the dynamics of bigeye tuna and its management. Model free (Perretti et al., 2013; Ward et al., 2014; see also Jabot, 2015) and machine learning-based approaches (e.g. Malde et al., 2019), may also contribute to improve our forecasts. These methods often outperform mechanistic models, at least for short lead times, providing an ideal candidate to complement the approach pursued here and develop multimodel ensemble forecasts.

The use of CPUE data also limits the interpretation of our results, and the approach would benefit from a more detailed assessment of potential changes in effort and catchability (e.g. Arreguín-Sánchez, 1996; Sharp, 1978). Longline catchability not only varies with changes in environmental conditions such as thermocline depth, which constrains the vertical distribution of bigeye tuna, or due to the impact of winds and surface currents on the depth of hooks (e.g. Bigelow et al., 2002; Domokos et al., 2007), but also with the availability and degree of spatial aggregation of prey (Bertrand et al., 2002). It has been recently found that changes in thermocline depth might account for up to one third of variability in bigeye tuna CPUE time series (Abascal et al., 2018), though the fluctuations manifest mainly at subseasonal scales (i.e. periods below 2 years). Longline CPUE gives an admittedly simple index of relative abundance, but various clues lend support to how we interpreted observed trends and environmental associations. Longline consistently captured large, adult bigeye tuna

according to recent assessments (Ducharme-Barth et al., 2020; Xu et al., 2020), which also point out declining trends and fluctuations consistent with those analysed in this study. Proposed regime shifts neither align with major changes in the regulation of the fisheries nor with changes in gear configuration, like the increase of hooks in the early 1990s (Xu et al., 2020). The regime shifts also involve prolonged excursions up to 25% above or below the mean trend, which clearly differ from short-lived, smaller deviations often associated with fluctuations in catchability (Abascal et al., 2018; Bigelow et al., 2002).

In light of increased stratification and prevailing declines in oxygen concentration through the world oceans (Breitburg et al., 2018; Sarmiento et al., 2004), our results reinforce the value of using mechanistically guided SDMs to monitor and analyse climate change impacts in large pelagics (Leung, Mislan, et al., 2019; Muhling et al., 2016; Stramma et al., 2011). In the case of bigeye tuna, the relationships found between temperature and oxygen through the water column and with primary productivity open the possibility to implement dynamic management practices that may facilitate anticipatory adjustments in harvest control rules and other management measures that could improve both economic and conservation outcomes (e.g. Tommasi, Stock, Pegion, et al., 2017). Biogeochemical data assimilation systems like ECDA-COBALT remain experimental (Park et al., 2018, 2019), but the growing availability of real-time, three-dimensional information about ocean biogeochemistry promises widely available operational products in the near future (Fennel et al., 2019). According to our results, these systems can foster the development of dedicated systems integrating biogeochemical information into ecological forecasts systems to implement efficient dynamic management strategies and promote the sustainable use of marine living resources.

AUTHOR CONTRIBUTIONS

ACKNOWLEDGEMENTS

CONFLICT OF INTEREST

The authors declare no conflict of interest.

DATA AVAILABILITY STATEMENT

Data available from the Dryad Digital Repository https://doi.org/10.5061/dryad.x3ffbg7p9 (Taboada et al., 2022). Bigeye tuna catch and effort was calculated based on the publicly available IATTC (www.iattc.org) and (www.wpcouncil.org) databases of tunas and billfishes.

ORCID

Fernando G. Taboada https://orcid.org/0000-0001-7634-887X
Jong-Yeon Park https://orcid.org/0000-0001-8125-4552
Barbara A. Muhling https://orcid.org/0000-0002-4555-6382
Desiree Tommasi https://orcid.org/0000-0003-4027-6047
Kisei R. Tanaka https://orcid.org/0000-0002-1901-6972
Ryan R. Rykaczewski https://orcid.org/0000-0001-8893-872X
Charles A. Stock https://orcid.org/0000-0001-9549-8013
Jorge L. Sarmiento https://orcid.org/0000-0001-5219-2604

REFERENCES

Abascal, F., Peatman, T., Leroy, B., Nicol, S., Schaefer, K., Fuller, D., & Hampton, J. (2018). Spatiotemporal variability in bigeye vertical distribution in the Pacific Ocean. *Fisheries Research*, *204*, 371–379. https://doi.org/10.1016/j.fshres.2018.03.013

Aksnes, D. L., Røstad, A., Kaartvedt, S., Martinez, U., Duarte, C. M., & Irigoien, X. (2017). Light penetration structures the deep acoustic scattering layers in the global ocean. *Science Advances*, *3*, e1602468. https://doi.org/10.1126/sciadv.1602468

Arreguín-Sánchez, F. (1996). Catchability: A key parameter for fish stock assessment. *Reviews in Fish Biology and Fisheries*, *6*. https://doi.org/10.1007/bf00182344

Arrizabalaga, H., Dufour, F., Kell, L., Merino, G., Ibaibarriaga, L., Chust, G., Irigoien, X., Santiago, J., Murua, H., Fraile, I., Chifflet, M., Goikoetxea, N., Sagarminaga, Y., Aumont, O., Bopp, L., Herrera, M., Fromentin, J. M., & Bonhomeau, S. (2015). Global habitat preferences of commercially valuable tuna. *Deep Sea Research Part II: Topical Studies in Oceanography*, *113*, 102–112. https://doi.org/10.1016/j.dsr2.2014.07.001

Barange, M., Bahri, T., Beveridge, M., Cochrane, K., Funge-Smith, S., & Poulain, F. (2018). *Impacts of climate change on fisheries and aquaculture: Synthesis of current knowledge, adaptation and mitigation options*. FAO Fisheries and Aquaculture technical paper 627.

Barton, A. D., Taboada, F. G., Atkinson, A., Widdicombe, C. E., & Stock, C. A. (2020). Integration of temporal environmental variation by the marine plankton community. *Marine Ecology Progess Series*, *647*, 1–16. https://doi.org/10.3354/meps13432

Bentlage, B., Peterson, A. T., Barve, N., & Cartwright, P. (2013). Plumbing the depths: Extending ecological niche modelling and species distribution modelling in three dimensions. *Global Ecology and Biogeography*, *22*, 952–961. https://doi.org/10.1111/geb.12049

Bernal, D., Brill, R. W., Dickson, K. A., & Shiels, H. A. (2017). Sharing the water column: Physiological mechanisms underlying species-specific habitat use in tunas. *Reviews in Fish Biology and Fisheries*, *27*, 843–880. https://doi.org/10.1007/s11160-017-9497-7

Bertrand, A., Josse, E., Bach, P., Gros, P., & Dagorn, L. (2002). Hydrological and trophic characteristics of tuna habitat: Consequences on tuna distribution and longline catchability. *Canadian Journal of Fisheries and Aquatic Sciences*, *59*, 1002–1013. https://doi.org/10.1139/f02-073

Bigelow, K. A., Hampton, J., & Miyabe, N. (2002). Application of a habitat-based model to estimate effective longline fishing effort and relative abundance of Pacific bigeye tuna (*Thunnus obesus*). *Fisheries Oceanography*, *11*, 143–155. https://doi.org/10.1046/j.1365-2419.2002.00196.x

Block, B. A., & Stevens, E. (2001). *Tuna: Physiology, ecology, and evolution, vol. 19 of fish physiology*. Academic Press. https://doi.org/10.1016/S1546-5098(01)19001-1

Breitburg, D., Levin, L. A., Oschlies, A., Grégoire, M., Chavez, F. P., Conley, D. J., Garçon, V., Gilbert, D., Gutiérrez, D., Isensee, K., Jacinto, G. S., Limburg, K. E., Montes, I., Naqvi, S. W. A., Pitcher, G. C., Rabalais, N. N., Roman, M. R., Rose, K. A., Seibel, B. A., … Zhang, J. (2018). Declining oxygen in the global ocean and coastal waters. *Science*, *359*, eaam7240. https://doi.org/10.1126/science.aam7240

Brill, R. W., Bigelow, K. A., Musyl, M. K., Fritsches, K. A., & Warrant, E. J. (2005). Bigeye tuna (*Thunnus obesus*) behavior and physiology and their relevance to stock assessments and fishery biology. *Collective Volume of Scientific Papers—ICCAT*, *57*, 142–161.

Brodie, S., Abrahms, B., Bograd, S. J., Carroll, G., Hazen, E. L., Muhling, B. A., Buil, M. P., Smith, J. A., Welch, H., & Jacox, M. G. (2021). Exploring timescales of predictability in species distributions. *Ecography*, *44*, 832–844. https://doi.org/10.1111/ecog.05504

Calkins, T. P. (1980). Synopsis of biological data on the bigeye tuna, *Thunus obesus* (Lowe, 1839), in the Pacific Ocean. In W. H. Bayliff (Ed.), *Synopses of biological data on eight species of Scombrids* (pp. 217–259). Inter-American Tropical Tuna Comission, Special Report No. 2.

Capotondi, A., Wittenberg, A. T., Kug, J. S., Takahashi, K., & McPhaden, M. J. (2020). ENSO diversity. In M. J. McPhaden, A. Santoso, & W. Cai (Eds.), *El Niño southern oscillation in a changing climate* (chap. 4, pp. 65–86). American Geophysical Union (AGU). https://doi.org/10.1002/9781119548164.ch4

Chavez, F. P., Ryan, J., Lluch-Cota, S. E., & Ñiquen, C. M. (2003). From anchovies to sardines and back: Multidecadal change in the Pacific Ocean. *Science*, *299*, 217–221. https://doi.org/10.1126/science.1075880

Cheung, W. W., Lam, V. W., Sarmiento, J. L., Kearney, K., Watson, R., & Pauly, D. (2009). Projecting global marine biodiversity impacts under climate change scenarios. *Fish and Fisheries*, *10*, 235–251. https://doi.org/10.1111/j.1467-2979.2008.00315.x

Cheung, W. W. L., Frölicher, T. L., Asch, R. G., Jones, M. C., Pinsky, M. L., Reygondeau, G., Rodgers, K. B., Rykaczewski, R. R., Sarmiento, J. L., Stock, C., & Watson, J. R. (2016). Building confidence in projections of the responses of living marine resources to climate change. *ICES Journal of Marine Science*, *73*, 1283–1296. https://doi.org/10.1093/icesjms/fsv250

Costello, C., Cao, L., Gelcich, S., Cisneros-Mata, M. Á., Free, C. M., Froehlich, H. E., Golden, C. D., Ishimura, G., Maier, J., Macadam-Somer, I., Mangin, T., Melnychuk, M. C., Miyahara, M., de Moor, C. L., Naylor, R., Nøstbakken, L., Ojea, E., O'Reilly, E., Parma, A. M., … Lubchenco, J. (2020). The future of food from the sea. *Nature*, *588*, 95–100. https://doi.org/10.1038/s41586-020-2616-y

Costello, C., Ovando, D., Clavelle, T., Strauss, C. K., Hilborn, R., Melnychuk, M. C., Branch, T. A., Gaines, S. D., Szuwalski, C. S., Cabral, R. B., Rader, D. N., & Leland, A. (2016). Global fishery prospects under contrasting management regimes. *Proceedings of the National Academy of Sciences of the United States of America*, *113*, 5125–5129. https://doi.org/10.1073/pnas.1520420113

Dagorn, L., Bach, P., & Josse, E. (2000). Movement patterns of large bigeye tuna (*Thunnus obesus*) in the open ocean, determined using ultrasonic telemetry. *Marine Biology*, *136*, 361–371. https://doi.org/10.1007/s002270050694

Dennis, B., & Taper, M. L. (1994). Density dependence in time series observations of natural populations: Estimation and testing. *Ecological Monographs*, *64*, 205–224. https://doi.org/10.2307/2937041

Deutsch, C., Berelson, W., Thunell, R., Weber, T., Tems, C., McManus, J., Crusius, J., Ito, T., Baumgartner, T., Ferreira, V., Mey, J., & van Geen, A. (2014). Centennial changes in North Pacific anoxia linked to tropical trade winds. *Science*, *345*, 665–668. https://doi.org/10.1126/science.1252332

Deutsch, C., Brix, H., Ito, T., Frenzel, H., & Thompson, L. (2011). Climate-forced variability of ocean hypoxia. *Science*, *333*, 336–339. https://doi.org/10.1126/science.1202422

Dewitte, B., Vazquez-Cuervo, J., Goubanova, K., Illig, S., Takahashi, K., Cambon, G., Purca, S., Correa, D., Gutierrez, D., Sifeddine, A., & Ortlieb, L. (2012). Change in el niño flavours over 1958–2008: Implications for the long-term trend of the upwelling off Peru. *Deep Sea Research Part II: Topical Studies in Oceanography*, *77–80*, 143–156. https://doi.org/10.1016/j.dsr2.2012.04.011

Di Lorenzo, E., & Ohman, M. D. (2013). A double-integration hypothesis to explain ocean ecosystem response to climate forcing. *Proceedings of the National Academy of Sciences of the United States of America*, *110*, 2496–2499. https://doi.org/10.1073/pnas.1218022110

Domokos, R., Seki, M. P., Polovina, J. J., & Hawn, D. R. (2007). Oceanographic investigation of the American Samoa albacore (*Thunnus alalunga*) habitat and longline fishing grounds. *Fisheries Oceanography*, *16*, 555–572. https://doi.org/10.1073/pnas.1218022110

Duarte, C. M., Agusti, S., Barbier, E., Britten, G. L., Castilla, J. C., Gattuso, J. P., Fulweiler, R. W., Hughes, T. P., Knowlton, N., Lovelock, C. E., Lotze, H. K., Predragovic, M., Poloczanska, E., Roberts, C., & Worm, B. (2020). Rebuilding marine life. *Nature*, *580*, 39–51. https://doi.org/10.1038/s41586-020-2146-7

Ducharme-Barth, N., Vincent, M., Hampton, J., Hamer, P., Williams, P., & Pilling, G. (2020). *Stock assessment of bigeye tuna in the western and Central Pacific Ocean*. Western and Central Pacific Fisheries Commission—WCPFC-SC16-2020/SA-WP-03 (REV3). http://www.wcpfc.int

Duffy, G., & Chown, S. (2017). Explicitly integrating a third dimension in marine species distribution modelling. *Marine Ecology Progess Series*, *564*, 1–8. https://doi.org/10.3354/meps12011

Enns, T., Scholander, P. F., & Bradstreet, E. D. (1965). Effect of hydrostatic pressure on gases dissolved in water. *Journal of Physical Chemistry*, *69*, 389–391. https://doi.org/10.1021/j100886a005

Espinoza-Morriberón, D., Echevin, V., Colas, F., Tam, J., Gutierrez, D., Graco, M., Ledesma, J., & Quispe-Ccalluari, C. (2019). Oxygen variability during ENSO in the Tropical South Eastern Pacific. *Frontiers of Marine Science*, *5*, 526. https://doi.org/10.3389/fmars.2018.00526

Eveson, J. P., Hobday, A. J., Hartog, J. R., Spillman, C. M., & Rough, K. M. (2015). Seasonal forecasting of tuna habitat in the great Australian bight. *Fisheries Research*, *170*, 39–49. https://doi.org/10.1016/j.fshres.2015.05.008

Fennel, K., Gehlen, M., Brasseur, P., Brown, C. W., Ciavatta, S., Cossarini, G., Crise, A., Edwards, C. A., Ford, D., Friedrichs, M. A. M., Gregoire, M., Jones, E., Kim, H. C., Lamouroux, J., Murtugudde, R., & Perruche, C. (2019). Advancing marine biogeochemical and ecosystem reanalyses and forecasts as tools for monitoring and managing ecosystem health. *Frontiers in Marine Science*, *6*. https://doi.org/10.3389/fmars.2019.00089

García, H. E., & Gordon, L. I. (1992). Oxygen solubility in seawater: Better fitting equations. *Limnology and Oceanography*, *37*, 1307–1312. https://doi.org/10.4319/lo.1992.37.6.1307

Gelman, A., Carlin, J. B., Stern, H. S., Dunson, D. B., Vehtari, A., & Rubin, D. B. (2014). *Bayesian data analysis* (3rd ed.). Chapman & Hall/CRC.

Gelman, A., & Rubin, D. B. (1992). Inference from iterative simulation using multiple sequences. *Statistical Science*, *7*, 457–472. https://doi.org/10.1214/ss/1177011136

Hare, S. R., & Mantua, N. J. (2000). Empirical evidence for north pacific regime shifts in 1977 and 1989. *Progress in Oceanography*, *47*, 103–145. https://doi.org/10.1016/S0079-6611(00)00033-1

Hastie, T., & Tibshirani, R. (1986). Generalized additive models. *Statistical Science*, 1, 297–310. https://doi.org/10.1214/ss/1177013604

Hobday, A. J., Hartog, J. R., Spillman, C. M., & Alves, O. (2011). Seasonal forecasting of tuna habitat for dynamic spatial management. *Canadian Journal of Fisheries and Aquatic Sciences*, 68, 898–911. https://doi.org/10.1139/f2011-031

Hobday, A. J., Spillman, C. M., Paige, J. E., & Hartog, J. R. (2016). Seasonal forecasting for decision support in marine fisheries and aquaculture. *Fisheries Oceanography*, 25, 45–56. https://doi.org/10.1111/fog.12083

Holland, K. N., Brill, R. W., Chang, R. K. C., Sibert, J. R., & Fournier, D. A. (1992). Physiological and behavioural thermoregulation in bigeye tuna (*Thunnus obesus*). *Nature*, 358, 410–412. https://doi.org/10.1038/358410a0

Hooten, M. B., & Hobbs, N. T. (2015). A guide to Bayesian model selection for ecologists. *Ecological Monographs*, 85, 3–28. https://doi.org/10.1890/14-0661.1

Hyndman, R. J., & Koehler, A. B. (2006). Another look at measures of forecast accuracy. *International Journal of Forecasting*, 22, 679–688. https://doi.org/10.1016/j.ijforecast.2006.03.001

ICCAT. (2006–2016). *ICCAT manual.* International Commission for the Conservation of Atlantic Tuna.

Jabot, F. (2015). Why preferring parametric forecasting to nonparametric methods? *Journal of Theoretical Biology*, 372, 205–210. https://doi.org/10.1016/j.jtbi.2014.07.038

Jacox, M. G., Alexander, M. A., Siedlecki, S., Chen, K., Kwon, Y. O., Brodie, S., Ortiz, I., Tommasi, D., & Widlansky, M. J. (2020). Seasonal-to-interannual prediction of north American coastal marine ecosystems: Forecast methods, mechanisms of predictability, and priority developments. *Progress in Oceanography*, 183, 102307. https://doi.org/10.1016/j.pocean.2020.102307

Juan-Jorda, M. J., Mosqueira, I., Cooper, A. B., Freire, J., & Dulvy, N. K. (2011). Global population trajectories of tunas and their relatives. *Proceedings of the National Academy of Sciences of the United States of America*, 108, 20650–20655. https://doi.org/10.1073/pnas.1107743108

Kaplan, I. C., Williams, G. D., Bond, N. A., Hermann, A. J., & Siedlecki, S. A. (2015). Cloudy with a chance of sardines: Forecasting sardine distributions using regional climate models. *Fisheries Oceanography*, 25, 15–27. https://doi.org/10.1111/fog.12131

Kume, S., & Schaefer, M. B. (1966). *Studies on the Japanese longline fishery for tuna and marlin in the Eastern Pacific Ocean*. Inter-American Tropical Tuna Commission (IATTC) Bulletin 3.

Lehodey, P., Senina, I., & Murtugudde, R. (2008). A spatial ecosystem and populations dynamics model (SEAPODYM)—Modeling of tuna and tuna-like populations. *Progress in Oceanography*, 78, 304–318. https://doi.org/10.1016/j.pocean.2008.06.004

Leung, S., Mislan, K. A. S., Muhling, B., & Brill, R. (2019). The significance of ocean deoxygenation for open ocean tunas and billfishes. In D. Laffoley & J. M. Baxter (Eds.), *Ocean deoxygenation: Everyones's problem* (chap. 8, pp. 277–308). IUCN, Global Marine and Polar Programme. https://doi.org/10.2305/IUCN.CH.2019.13.en

Leung, S., Thompson, L., McPhaden, M. J., & Mislan, K. A. S. (2019). ENSO drives near-surface oxygen and vertical habitat variability in the tropical Pacific. *Environmental Research Letters*, 14, 064020. https://doi.org/10.1088/1748-9326/ab1c13

Lindeløv, J. K. (2020). *Mcp: An r package for regression with multiple change points*. https://doi.org/10.31219/osf.io/fzqxv

Lowe, T. E., Brill, R. W., & Cousins, K. L. (2000). Blood oxygen-binding characteristics of bigeye tuna (*Thunnus obesus*), a high-energy-demand teleost that is tolerant of low ambient oxygen. *Marine Biology*, 136, 1087–1098. https://doi.org/10.1007/s002270000255

Malde, K., Handegard, N. O., Eikvil, L., & Salberg, A. B. (2019). Machine intelligence and the data-driven future of marine science. *ICES Journal of Marine Science*, 77, 1274–1285. https://doi.org/10.1093/icesjms/fsz057

Maunder, M. N., Sibert, J. R., Fonteneau, A., Hampton, J., Kleiber, P., & Harley, S. J. (2006). Interpreting catch per unit effort data to assess the status of individual stocks and communities. *ICES Journal of Marine Science*, 63, 1373–1385. https://doi.org/10.1016/j.icesjms.2006.05.008

Maxwell, S. M., Hazen, E. L., Lewison, R. L., Dunn, D. C., Bailey, H., Bograd, S. J., Briscoe, D. K., Fossette, S., Hobday, A. J., Bennett, M., Benson, S., Caldwell, M. R., Costa, D. P., Dewar, H., Eguchi, T., Hazen, L., Kohin, S., Sippel, T., & Crowder, L. B. (2015). Dynamic Ocean management: Defining and conceptualizing real-time management of the ocean. *Marine Policy*, 58, 42–50. https://doi.org/10.1016/j.marpol.2015.03.014

McCluney, J. K., Anderson, C. M., & Anderson, J. L. (2019). The fishery performance indicators for global tuna fisheries. *Nature Communications*, 10, 1641. https://doi.org/10.1038/s41467-019-09466-6

Meehl, G. A., Richter, J. H., Teng, H., Capotondi, A., Cobb, K., Doblas-Reyes, F., Donat, M. G., England, M. H., Fyfe, J. C., Han, W., Kim, H., Kirtman, B. P., Kushnir, Y., Lovenduski, N. S., Mann, M. E., Merryfield, W. J., Nieves, V., Pegion, K., Rosenbloom, N., … Xie, S. P. (2021). Initialized earth system prediction from subseasonal to decadal timescales. *Nature Reviews Earth & Environment*, 2, 340–357. https://doi.org/10.1038/s43017-021-00155-x

Mislan, K. A. S., Deutsch, C. A., Brill, R. W., Dunne, J. P., & Sarmiento, J. L. (2017). Projections of climate-driven changes in tuna vertical habitat based on species-specific differences in blood oxygen affinity. *Global Change Biology*, 23, 4019–4028. https://doi.org/10.1111/gcb.13799

Muhling, B. A., Brill, R., Lamkin, J. T., Roffer, M. A., Lee, S. K., Liu, Y., & Muller-Karger, F. (2016). Projections of future habitat use by Atlantic bluefin tuna: Mechanistic vs. correlative distribution models. *ICES Journal of Marine Science*, 74, 698–716. https://doi.org/10.1093/icesjms/fsw215

Murdoch, W. W., Kendall, B. E., Nisbet, R. M., Briggs, C. J., McCauley, E., & Bolser, R. (2002). Single-species models for many-species food webs. *Nature*, 417, 541–543. https://doi.org/10.1038/417541a

Musyl, M. K., Brill, R. W., Boggs, C. H., Curran, D. S., Kazama, T. K., & Seki, M. P. (2003). Vertical movements of bigeye tuna (*Thunnus obesus*) associated with islands, buoys, and seamounts near the main Hawaiian islands from archival tagging data. *Fisheries Oceanography*, 12, 152–169. https://doi.org/10.1046/j.1365-2419.2003.00229.x

Myers, R. A., & Worm, B. (2003). Rapid worldwide depletion of predatory fish communities. *Nature*, 423, 280–283. https://doi.org/10.1038/nature01610

Newman, M., Alexander, M. A., Ault, T. R., Cobb, K. M., Deser, C., Lorenzo, E. D., Mantua, N. J., Miller, A. J., Minobe, S., Nakamura, H., Schneider, N., Vimont, D. J., Phillips, A. S., Scott, J. D., & Smith, C. A. (2016). The Pacific decadal oscillation, revisited. *Journal of Climate*, 29, 4399–4427. https://doi.org/10.1175/JCLI-D-15-0508.1

Olson, R., Young, J., Ménard, F., Potier, M., Allain, V., Goñi, N., Logan, J., & Galván-Magaña, F. (2016). Bioenergetics, trophic ecology, and niche separation of tunas. *Advances in Marine Biology*, 74, 199–344. https://doi.org/10.1016/bs.amb.2016.06.002

Park, J. Y., Stock, C. A., Dunne, J. P., Yang, X., & Rosati, A. (2019). Seasonal to multiannual marine ecosystem prediction with a global earth system model. *Science*, 365, 284–288. https://doi.org/10.1126/science.aav6634

Park, J. Y., Stock, C. A., Yang, X., Dunne, J. P., Rosati, A., John, J., & Zhang, S. (2018). Modeling global ocean biogeochemistry with physical data assimilation: A pragmatic solution to the equatorial instability. *Journal of Advances in Modeling Earth Systems*, 10, 891–906. https://doi.org/10.1002/2017ms001223

Payne, M. R., Hobday, A. J., MacKenzie, B. R., Tommasi, D., Dempsey, D. P., Fässler, S. M. M., Haynie, A. C., Ji, R., Liu, G., Lynch, P. D., Matei, D., Miesner, A. K., Mills, K. E., Strand, K. O., & Villarino, E. (2017). Lessons from the first generation of marine ecological forecast products. *Frontiers in Marine Science*, 4. https://doi.org/10.3389/fmars.2017.00289

Perretti, C. T., Munch, S. B., & Sugihara, G. (2013). Model-free forecasting outperforms the correct mechanistic model for simulated and experimental data. *Proceedings of the National Academy of Sciences of the United States of America*, 110, 5253–5257. https://doi.org/10.1073/pnas.1216076110

Pickens, B. A., Carroll, R., Schirripa, M. J., Forrestal, F., Friedland, K. D., & Taylor, J. C. (2021). A systematic review of spatial habitat associations and modeling of marine fish distribution: A guide to predictors, methods, and knowledge gaps. *PLoS ONE*, 16, e0251818. https://doi.org/10.1371/journal.pone.0251818

Plummer, M. (2003). JAGS: A program for analysis of Bayesian graphical models using Gibbs sampling. Proceedings of the 3rd international workshop on Distributed Statistical Computing (DSC 2003), FAO Fisheries Report, pp. 1065–1080, ISSN 1609-395X, Vienna, Austria.

Post, V., & Squires, D. (2020). Managing bigeye tuna in the western and Central Pacific Ocean. *Frontiers in Marine Science*, 7. https://doi.org/10.3389/fmars.2020.00619

R Core Team. (2021). *R: A language and environment for statistical computing*. R Foundation for Statistical Computing.

Reglero, P., Tittensor, D., Álvarez-Berastegui, D., Aparicio-González, A., & Worm, B. (2014). Worldwide distributions of tuna larvae: Revisiting hypotheses on environmental requirements for spawning habitats. *Marine Ecology Progress Series*, 501, 207–224. https://doi.org/10.3354/meps10666

Robinson, L. M., Elith, J., Hobday, A. J., Pearson, R. G., Kendall, B. E., Possingham, H. P., & Richardson, A. J. (2011). Pushing the limits in marine species distribution modelling: Lessons from the land present challenges and opportunities. *ICES Journal of Marine Science*, 20, 789–802. https://doi.org/10.1111/j.1466-8238.2010.00636.x

Rooker, J. R., Wells, R. J. D., Itano, D. G., Thorrold, S. R., & Lee, J. M. (2016). Natal origin and population connectivity of bigeye and yellowfin tuna in the Pacific Ocean. *Fisheries Oceanography*, 25, 277–291. https://doi.org/10.1111/fog.12154

Rouyer, T., Sadykov, A., Ohlberger, J., & Stenseth, N. C. (2012). Does increasing mortality change the response of fish populations to environmental fluctuations? *Ecology Letters*, 15, 658–665. https://doi.org/10.1111/j.1461-0248.2012.01781.x

Rudnick, D. L., & Davis, R. E. (2003). Red noise and regime shifts. *Deep Sea Research Part I: Oceanographic Research Papers*, 50, 691–699. https://doi.org/10.1016/S0967-0637(03)00053-0

Sarmiento, J. L., Slater, R., Barber, R., Bopp, L., Doney, S. C., Hirst, A. C., Kleypas, J., Matear, R., Mikolajewicz, U., Monfray, P., Soldatov, V., Spall, S. A., & Stouffer, R. (2004). Response of ocean ecosystems to climate warming. *Global Biogeochem Cycles*, 18, GB3003. https://doi.org/10.1029/2003GB002134

Satoh, K., Xu, H., Minte-Vera, C. V., Maunder, M. N., & Kitakado, T. (2021). Size-specific spatiotemporal dynamics of bigeye tuna (*Thunnus obesus*) caught by the longline fishery in the eastern Pacific Ocean. *Fisheries Research*, 243, 106065. https://doi.org/10.1016/j.fshres.2021.106065

Schaefer, K., Fuller, D., Hampton, J., Caillot, S., Leroy, B., & Itano, D. (2015). Movements, dispersion, and mixing of bigeye tuna (*Thunnus obesus*) tagged and released in the equatorial Central Pacific Ocean, with conventional and archival tags. *Fisheries Research*, 161, 336–355. https://doi.org/10.1016/j.fshres.2014.08.018

Schaefer, K. M. (2010). Reproductive biology of tunas. *Fish Physiology*, 19, 225–270. https://doi.org/10.1016/s1546-5098(01)19007-2

Schaefer, K. M., & Fuller, D. W. (2010). Vertical movements, behavior, and habitat of bigeye tuna (*Thunnus obesus*) in the equatorial eastern Pacific Ocean, ascertained from archival tag data. *Marine Biology*, 157, 2625–2642. https://doi.org/10.1007/s00227-010-1524-3

Schaefer, K. M., Fuller, D. W., & Block, B. A. (2009). Vertical movements and habitat utilization of skipjack (*Katsuwonus pelamis*), Yellowfin (*Thunnus albacares*), and bigeye (*Thunnus obesus*) tunas in the equatorial eastern Pacific Ocean, ascertained through archival tag data. In J. L. Nielsen, H. Arrizabalaga, N. Fragoso, A. Hobday, M. Lutcavage, & J. Sibert (Eds.), *Tagging and tracking of marine animals with electronic devices. Reviews: Methods and technologies in fish biology and fisheries* (pp. 121–144). Springer. https://doi.org/10.1007/978-1-4020-9640-2_8

Schmidt, J. O., Bograd, S. J., Arrizabalaga, H., Azevedo, J. L., Barbeaux, S. J., Barth, J. A., Boyer, T., Brodie, S., Cárdenas, J. J., Cross, S., Druon, J. N., Fransson, A., Hartog, J., Hazen, E. L., Hobday, A., Jacox, M., Karstensen, J., Kupschus, S., Lopez, J., ... Zawislak, P. A. (2019). Future Ocean observations to connect climate, fisheries and marine ecosystems. *Frontiers in Marine Science*, 6. https://doi.org/10.3389/fmars.2019.00550

Seferian, R., Bopp, L., Gehlen, M., Swingedouw, D., Mignot, J., Guilyardi, E., & Servonnat, J. (2014). Multiyear predictability of tropical marine productivity. *Proceedings of the National Academy of Sciences of the United States of America*, 111, 11646–11651. https://doi.org/10.1073/pnas.1315855111

Sharp, G. D. (1978). Behavioral and physiological properties of tunas and their effects on vulnerability to fishing gear. In G. D. Sharp & A. E. Dizon (Eds.), *The physiological ecology of tunas* (pp. 397–449). Academic Press. https://doi.org/10.1016/b978-0-12-639180-0.50032-x

Sharp, G. D. (1995). It's about time: New beginnings and old good ideas in fisheries science. *Fisheries Oceanography*, 4, 324–341. https://doi.org/10.1111/j.1365-2419.1995.tb00077.x

Sibert, J., Hampton, J., Kleiber, P., & Maunder, M. (2006). Biomass, size, and trophic status of top predators in the Pacific Ocean. *Science*, 314, 1773–1776. https://doi.org/10.1126/science.1135347

Skern-Mauritzen, M., Ottersen, G., Handegard, N. O., Huse, G., Dingsør, G. E., Stenseth, N. C., & Kjesbu, O. S. (2016). Ecosystem processes are rarely included in tactical fisheries management. *Fish and Fisheries*, 17, 165–175. https://doi.org/10.1111/faf.12111

Stock, C. A., Alexander, M. A., Bond, N. A., Brander, K. M., Cheung, W. W., Curchitser, E. N., Delworth, T. L., Dunne, J. P., Griffies, S. M., Haltuch, M. A., Hare, J. A., Hollowed, A. B., Lehodey, P., Levin, S. A., Link, J. S., Rose, K. A., Rykaczewski, R. R., Sarmiento, J. L., Stouffer, R. J., ... Werner, F. E. (2011). On the use of ipcc-class models to assess the impact of climate on living marine resources. *Progress in Oceanography*, 88, 1–27. https://doi.org/10.1016/j.pocean.2010.09.001

Stock, C. A., Dunne, J. P., & John, J. G. (2014). Global-scale carbon and energy flows through the marine planktonic food web: An analysis with a coupled physical–biological model. *Progress in Oceanography*, 120, 1–28. https://doi.org/10.1016/j.pocean.2013.07.001

Stock, C. A., John, J. G., Rykaczewski, R. R., Asch, R. G., Cheung, W. W. L., Dunne, J. P., Friedland, K. D., Lam, V. W. Y., Sarmiento, J. L., & Watson, R. A. (2017). Reconciling fisheries catch and ocean productivity. *Proceedings of the National Academy of Sciences of the United States of America*, 114, E1441–E1449. https://doi.org/10.1073/pnas.1610238114

Stramma, L., Prince, E. D., Schmidtko, S., Luo, J., Hoolihan, J. P., Visbeck, M., Wallace, D. W. R., Brandt, P., & Körtzinger, A. (2011). Expansion of oxygen minimum zones may reduce available habitat for tropical pelagic fishes. *Nature Climate Change*, 2, 33–37. https://doi.org/10.1038/nclimate1304

Taboada, F. G. (2019). Understanding variability in marine fisheries: Importance of environmental forcing. In *Sustainability of ocean and human systems amidst global environmental change* (pp. 149–163). Elsevier. https://doi.org/10.1016/b978-0-12-817945-1.00014-9

Taboada, F. G., Barton, A. D., Stock, C. A., Dunne, J., & John, J. G. (2019). Seasonal to interannual predictability of oceanic net primary production inferred from satellite observations. *Progress in Oceanography*, *170*, 28–39. https://doi.org/10.1016/j.pocean.2018.10.010

Taboada, F. G., Park, J. Y., Muhling, B. A., Tommasi, D., Tanaka, K. R., Rykaczewski, R. R., Stock, C. A., & Sarmiento, J. L. (2022). Data from: Anticipating fluctuations of bigeye tuna in the Pacific Ocean from three-dimensional ocean biogeochemistry. *Dryad Digital Repository*, https://doi.org/10.5061/dryad.x3fbg7p9

Thygesen, U. H., Sommer, L., Evans, K., & Patterson, T. A. (2016). Dynamic optimal foraging theory explains vertical migrations of bigeye tuna. *Ecology*, *97*, 1852–1861. https://doi.org/10.1890/15-1130.1

Tommasi, D., Stock, C. A., Hobday, A. J., Methot, R., Kaplan, I. C., Eveson, J. P., Holsman, K., Miller, T. J., Gaichas, S., Gehlen, M., Pershing, A., Vecchi, G. A., Msadek, R., Delworth, T., Eakin, C. M., Haltuch, M. A., Séférian, R., Spillman, C. M., Hartog, J. R., ... Werner, F. E. (2017). Managing living marine resources in a dynamic environment: The role of seasonal to decadal climate forecasts. *Progress in Oceanography*, *152*, 15–49. https://doi.org/10.1016/j.pocean.2016.12.011

Tommasi, D., Stock, C. A., Pegion, K., Vecchi, G. A., Methot, R. D., Alexander, M. A., & Checkley, D. M. (2017). Improved management of small pelagic fisheries through seasonal climate prediction. *Ecological Applications*, *27*, 378–388. https://doi.org/10.1002/eap.1458

Turchin, P. (2003). *Complex population dynamics. A theoretical/empirical synthesis, vol. 25 of monographs in population biology.* Princeton University Press. https://doi.org/10.1515/9781400847280

Ward, E. J., Holmes, E. E., Thorson, J. T., & Collen, B. (2014). Complexity is costly: A meta-analysis of parametric and non-parametric methods for short-term population forecasting. *Oikos*, *123*, 652–661. https://doi.org/10.1111/j.1600-0706.2014.00916.x

Watanabe, S. (2013). A widely applicable Bayesian information criterion. *Journal of Machine Learning Research*, *14*, 867–897.

Weatherton, L. V., Magnan, A. K., Rogers, A. D., Sumaila, U. R., & Cheung, W. W. L. (2016). Observed and projected impacts of climate change on marine fisheries, aquaculture, coastal tourism, and human health: An update. *Frontiers of Marine Science*, *3*, 48. https://doi.org/10.3389/fmars.2016.00048

Wood, S. N. (2016). Just another Gibbs additive modeler: Interfacing *JAGS* and *mgcv*. *Journal of Statistical Software*, *75*, 1–15. https://doi.org/10.18637/jss.v075.i07

Wood, S. N. (2017). *Generalized additive models. Texts in statistical science* (2nd ed.). Chapman and Hall/CRC. https://doi.org/10.1201/9781315370279

Woodworth-Jefcoats, P. A., & Wren, J. L. K. (2020). Toward an environmental predictor of tuna recruitment. *Fisheries Oceanography*, *29*, 436–441. https://doi.org/10.1111/fog.12487

Xu, H., Maunder, M. N., Minte-Vera, C., Valero, J. L., Lennert-Cody, C., & Aires-da-Silva, A. (2020). *Bigeye tuna in the eastern Pacific Ocean, 2019: Benchmark assessment.* Inter-American Tropical Tuna Commission, Scientific Advisory Committee 11th meeting, La Jolla, CA, USA.

Zhang, S., Harrison, M. J., Rosati, A., & Wittenberg, A. (2007). System design and evaluation of coupled ensemble data assimilation for global oceanic climate studies. *Monthly Weather Review*, *135*, 3541–3564. https://doi.org/10.1175/mwr3466.1

Zhang, T., Song, L., Yuan, H., Song, B., & Ngando, N. E. (2021). A comparative study on habitat models for adult bigeye tuna in the Indian Ocean based on gridded tuna longline fishery data. *Fisheries Oceanography*, *30*, 584–607. https://doi.org/10.1111/fog.12539

Zhou, C., Wan, R., Cao, J., Xu, L., Wang, X., & Zhu, J. (2020). Spatial variability of bigeye tuna habitat in the Pacific Ocean: Hindcast from a refined ecological niche model. *Fisheries Oceanography*, *30*, 23–37. https://doi.org/10.1111/fog.12500

SUPPORTING INFORMATION

Additional supporting information can be found online in the Supporting Information section at the end of this article.